

A WDM-PON with an 80 Gb/s capacity based on wavelength-locked Fabry-Perot laser diode

Hoon-Keun Lee,¹ Ho-Sung Cho,² Joon-Young Kim,¹ and Chang-Hee Lee^{1,*}

¹Division of Electrical Engineering, Korea Advanced Institute of Science and Technology, 373-1, Guseong-dong, Yuseong-gu, Daejeon, 305-701, Korea

²Eldis Inc. 958-3, Daechon-dong, Buk-gu, Gwangju, 500-706, Korea

*changheelee@kaist.edu

Abstract: We investigate a high capacity WDM-PON based on wavelength-locked Fabry-Perot laser diodes. A color-free transmission of 2.5 Gb/s per channel is achieved with a polarization independent F-P LD and a decision threshold control circuit at the receiver. Then, we demonstrate an 80 Gb/s capacity (2.5 Gb/s \times 32 channels) WDM-PON with transmission length of 20 km. We also investigate impairments in transmission.

©2010 Optical Society of America

OCIS codes: (060.4510) Optical communications; (060.4250) Networks.

References and links

1. C.-H. Lee, W. V. Sorin, and B. Y. Kim, "Fiber to the Home using a PON Infrastructure," *J. Lightwave Technol.* **24**(12), 4568–4583 (2006).
2. C.-H. Lee, S.-M. Lee, K.-M. Choi, J.-H. Moon, S.-G. Mun, K.-T. Jeong, J. H. Kim, and B. Kim, "WDM-PON experiences in Korea [Invited]," *J. Opt. Netw.* **6**(5), 451–464 (2007).
3. S.-G. Mun, J.-H. Moon, H.-K. Lee, J.-Y. Kim, and C.-H. Lee, "A WDM-PON with a 40 Gb/s (32 \times 1.25 Gb/s) capacity based on wavelength-locked Fabry-Perot laser diodes," *Opt. Express* **16**(15), 11361–11368 (2008).
4. J. S. Jeong, and C.-H. Lee, "Optical Noise Suppression Techniques for Wavelength-Locked Fabry-Perot Laser Diode," in *Proceedings of the 15th Asia-Pacific Conference on Communications* (Shanghai, China, 2009), Paper 142.
5. A. D. McCoy, P. Horak, B. C. Thomsen, M. Ibsen, and D. J. Richardson, "Noise Suppression of Incoherent Light Using a Gain-Saturated SOA: Implications for Spectrum-Sliced WDM Systems," *J. Lightwave Technol.* **23**(8), 2399–2409 (2005).
6. A. Shen, D. Make, F. Poingt, L. Legouezigou, F. Pommereau, O. Legouezigou, J. Landreau, B. Rousseau, F. Lelarge, and G.-H. Daun, "Polarisation insensitive injection locked Fabry-Perot laser diodes for 2.5Gb/s WDM access applications," in *Proceedings of the European Conference and Exhibition on Optical Communication* (Brussels, Belgium, 2008), Paper Th.3.D.1.
7. H.-S. Kim, B.-S. Choi, K.-S. Kim, D. C. Kim, O.-K. Kwon, and D.-K. Oh, "Multisection RSOA for 2.5 Gbps Colorless WDM-PON," in *Proceedings of the European Conference and Exhibition on Optical Communication* (Vienna, Austria, 2009), Paper P2.17.
8. J.-H. Moon, K.-M. Choi, S.-G. Mun, and C.-H. Lee, "Effects of Back-Reflection in WDM-PONs Based on Seed Light Injection," *IEEE Photon. Technol. Lett.* **19**(24), 2045–2047 (2007).
9. H.-K. Lee, J.-H. Moon, S.-G. Mun, K.-M. Choi, and C.-H. Lee, "Decision Threshold Control Method for the Optical Receiver of a WDM-PON," *J. Opt. Commun. Netw.* **2**(6), 381–388 (2010).
10. J. C. Palais, *Fiber Optic Communications, 5th ed.* (Pearson Prentice-Hall, 2005), Chap. 11.
11. W. Lee, M. Y. Park, S. H. Cho, J. Lee, C. Kim, G. Jeong, and B. W. Kim, "Bidirectional WDM-PON Based on Gain-Saturated Reflective Semiconductor Optical Amplifiers," *IEEE Photon. Technol. Lett.* **17**(11), 2460–2462 (2005).
12. A. D. McCoy, B. C. Thomsen, M. Ibsen, and D. J. Richardson, "Filtering Effects in a Spectrum-Sliced WDM System Using SOA-based Noise Reduction," *IEEE Photon. Technol. Lett.* **16**(2), 680–682 (2004).
13. S.-H. Cho, H.-H. Lee, M.-Y. Park, J.-H. Lee, J.-H. Yu, and B. Kim, "Effects of RSOA Gain Ripples on Upstream Transmission in a SML-Seeded Loop-Back WDM-PON," in *Proceedings of the Optical Fiber Communication Conference* (San Diego, CA, 2009), Paper JWA70.
14. K.-Y. Park, and C.-H. Lee, "Intensity Noise in a Wavelength-Locked Fabry-Perot Laser Diode to a Spectrum Sliced ASE," *IEEE J. Quantum Electron.* **44**(3), 209–215 (2008).
15. J.-Y. Kim, S.-G. Mun, J.-H. Moon, H.-K. Lee, and C.-H. Lee, "A High Capacity and Long Reach DWDM-PON Using Triple-Contact F-P LDs," in *Proceedings of the Optical Fiber Communication Conference* (San Diego, CA, 2010), Paper JThA31.

1. Introduction

Recently, bandwidth requirements for subscribers are explosively increased with growth of video-centric services such as Internet Protocol Television (IPTV), High Definition Television (HDTV), 3-D TV. To accommodate these bandwidth intensive services in access network, a wavelength division multiplexing passive optical network (WDM-PON) has been attracted considerable attention because of its large bandwidth, high security, and protocol transparency [1]. A WDM-PON based on wavelength-locked Fabry-Perot laser diodes (F-P LDs) was proposed and it has been already commercialized [2]. The wavelength-locked F-P LD is attractive because of its cost-effective color-free (or colorless) feature. However, the high-speed transmission (> 2.5 Gb/s per channel) is limited by the optical beat noises (or intensity noises) resulting from the injected spectrum-sliced amplified spontaneous emission (ASE) light [3]. This beat noise can be reduced by increasing the spectrum-sliced ASE bandwidth and/or noise suppression technique [4]. However, increase of ASE bandwidth reduces number of transmission channels and increases dispersion penalty. The noise suppression scheme makes the WDM-PON architecture complicated and imposes an additional cost on the subscribers. Moreover, it brings about dispersion induced de-correlation penalty [4,5]. The beat noise can be also reduced by injecting a coherent seed light instead of the incoherent (ASE) seed light. So far, 2.5 Gb/s transmission has been demonstrated with a coherent seeded light injection to polarization independent (PI) F-P LDs [6]/reflective semiconductor optical amplifiers (RSOAs) [7]. However, optical back reflection induced impairments are hurdles for a low cost and high performance system [8].

In this paper, we present 2.5 Gb/s operation for the WDM-PON based on the wavelength-locked F-P LD at 100 GHz channel spacing with ASE seeding. The intensity noise was reduced by a factor of 2 with a PI F-P LD. It enables 2.5 Gb/s per channel WDM-PON with help of decision threshold control. We also demonstrate a WDM-PON with an 80-Gb/s capacity over a conventional C band. The dominant system impairment after transmission was dispersion induced de-correlation of intensity noise suppressed light.

2. Considerations for 2.5 Gb/s transmission

2.1 RIN requirement

The ultimate performance of the WDM-PON based on wavelength-locked F-P LD is limited by the relative intensity noise (RIN) resulting from the spectrum slicing of the broadband seed light [3,9]. Assuming a RIN value is x (< 0) dB/Hz, the RIN-induced noise power can be given by [10]

$$\sigma_{RIN}^2 = R^2 \cdot P^2 \cdot 10^{\frac{x}{10}} \cdot B_e \quad (1)$$

where, R is the receiver responsivity, P is the optical received power and B_e is the electrical bandwidth of the receiver. For 1.25 Gb/s data rate, the required RIN level was around -110 dB/Hz for error-free transmission [9]. It may be noted that we need to set the decision threshold level of the optical receiver near the optimum value. When a broadband light source (BLS) such as a PI ASE light was spectrum-sliced by a 100 GHz flat-top type arrayed waveguide grating (AWG), the measured RIN was about -110 dB/Hz. Thus we have to suppress the RIN level more than 3 dB for 2.5 Gb/s transmission at 100 GHz channel spacing [10]. A gain saturation characteristic in an F-P LD [4] or an RSOA [11] can be used for the noise suppression. However, in WDM-PON, the noise suppressed signal is degraded after

passing through the 2 AWGs located at the central office (CO) and remote node (RN). This is so called optical filtering effect [12].

2.2 Dispersion and phase de-correlation effects

Beside of RIN requirement in the previous Section, we need to consider dispersion induced penalty for high speed data transmission. The dispersion penalty will be much serious in transmission of a high speed spectrum-sliced ASE signal, since the spectral width is comparable to the bandwidth of the filter (AWG) used for the spectrum slicing. The dispersion penalty can be reduced by reducing the filter bandwidth. However, the RIN increases as we decrease the bandwidth. Thus we have to suppress the RIN for a high speed WDM-PON with a high channel count. Unfortunately, transmission of the noise suppressed spectrum-sliced signal brings about an additional penalty. The dispersion induces wavelength dependent phase shift to the noise suppressed signal [4,5]. As a result, the noise suppression effects are diminished. It brings about additional penalty on top of the well known dispersion penalty. Thus the RIN requirement will be tighter, when we consider the dispersion in the transmission fiber.

3. Experiment results

3.1 Experimental setups

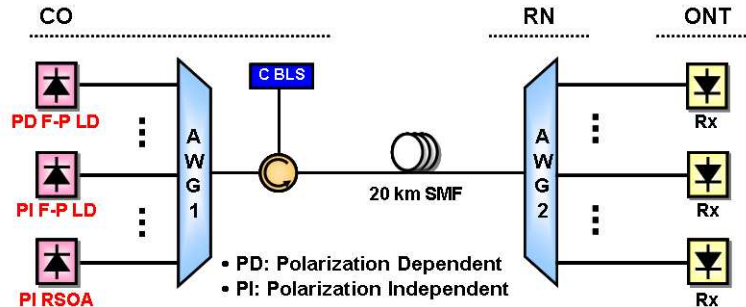


Fig. 1. Experimental setup for 2.5 Gb/s transmission.

The experimental setup based on the wavelength-locked F-P LDs to demonstrate 2.5 Gb/s transmission is shown in Fig. 1. The BLS output (ASE light) was spectrum-sliced by an AWG1 and injected into the polarization dependent (PD) F-P LD and the PI F-P LD located at the CO via an optical circulator. Then the output signal of the wavelength-locked F-P LDs were sent to the AWG2 located at the RN after passing through the AWG1 and 20 km single mode fiber (SMF). At the optical network terminal (ONT), a PIN-PD based receiver was employed with a decision threshold control circuit to enhance receiver performance. The channel spacing and 3-dB bandwidth of the AWG were 100 GHz (0.8 nm) and 80 GHz (0.64 nm), respectively. The F-P LDs were directly modulated at 2.5 Gb/s NRZ data with pseudorandom bit sequence (PRBS) pattern length of 2^7-1 . The mode spacing and the front facet reflectivity of the F-P LDs were about 0.56 nm and 0.1%, respectively. The PD F-P LD was made by a quantum well active medium and the PI F-P LD was made by a tensile strained InGaAsP bulk active medium. These were operated at the bias current of $2.0 I_{th}$, where I_{th} is the lasing threshold current. In this experiment, a PI RSOA was used for comparison. The RSOA was also made of a tensile strained InGaAsP bulk material. It consisted of a 500 μm active waveguide section and a 400 μm passive waveguide section including a 7° tilted spot size converter. The F-P LDs and RSOA were packaged with a conventional transistor outlook (TO)-can type. It may be noted that we used downstream transmission to provide a sufficient injection power to the F-P LDs.

3.2 RIN suppression of a spectrum-sliced ASE light

As mentioned before, we need the RIN suppression for 2.5 Gb/s signal transmission at 100 GHz channel spacing. To investigate the noise suppression effects, we measured RIN according to the ASE injection power. These measured RIN are shown in Fig. 2 for both the PD F-P LD case (■: best case, □: worst case) and the PI F-P LD case (▲: best case, △: worst case). The best case was observed when the injection wavelength is close to the one of the lasing mode, while the worst case when the injection wavelength is located middle of the two modes. The RIN measurements were performed by using an electrical spectrum analyzer (ESA) and an avalanche photo detector (APD). It was measured within the frequency span of 50 MHz ~1.5 GHz by averaging the measured values of 10 times. The RIN values were evaluated at ONT in Fig. 1 to take into consideration of a real WDM-PON. However, we did not insert the feeder fiber and the distribution fiber to investigate the noise suppression by the F-P LDs only. The RIN suppression increases as increasing the ASE injection power. Moreover, the PI F-P LD has about 3 dB less noise compared with the PD F-P LD both the best case and the worst case. This result implies that the data rate can be increased twice by using the PI F-P LD. As shown in the measured results, the noise reduction effect was saturated from the injection power of -4 dBm. Thus, we selected the maximum injection power -4 dBm for experiments.

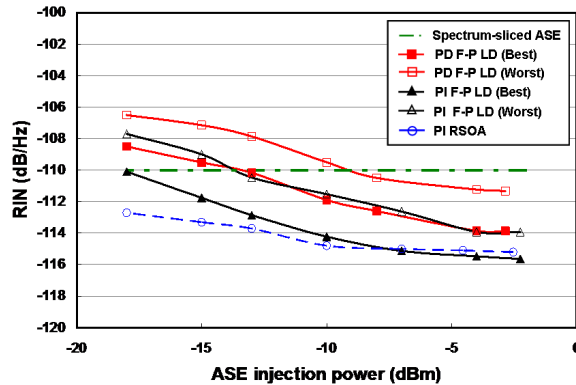


Fig. 2. Comparison of the noise reduction effects according to ASE injection power.

We also show the measured RIN of the PI RSOA (○) for comparison. At low injection power, the RSOA showed lower RIN compared with the F-P LDs. This can be explained by both the low polarization dependent gain (PDG) of less than 1 dB and the low spectral ripple. However, at high injection power, the best case RIN of the PI F-P LD was lower than that of the RSOA. To investigate the origin of this feature, we measured the PDG of the PI F-P LD as shown in Fig. 3. The measured light output-current (L-I) curve in Fig. 3(a) shows almost polarization independent output power for both orthogonal polarizations. However, it rapidly increases above the lasing threshold. The nature of polarization dependency can be explained by the polarization dependent loss, mainly resulting from the mirror reflectivity, and the polarization dependent cavity confinement factor. It is well known that a small difference of gain/loss will give a big difference in output power, when the laser operates above the lasing threshold. It may be noted that this laser is not optimized to have the same reflectivity for both polarization.

We also measured the PDG of the laser according to ASE injection power as shown in Fig. 3(b). For this measurement, the laser was biased around $2.0 I_{th}$. When the injection power is low, the laser operates above the lasing threshold. Thus, we have a high PDG. However, the PDG decreased rapidly as the ASE injection power increased. The carrier density in the active region of the laser was depleted below the lasing threshold with a high ASE injection power.

Thus the laser operates below the lasing threshold. It brings about decreases of the PDG. In this region, the characteristics of the antireflection coated PI F-P LD was very similar to that of a RSOA with a finite reflectivity. To confirm this, we showed the measured PDG for the RSOA in Fig. 3(b).

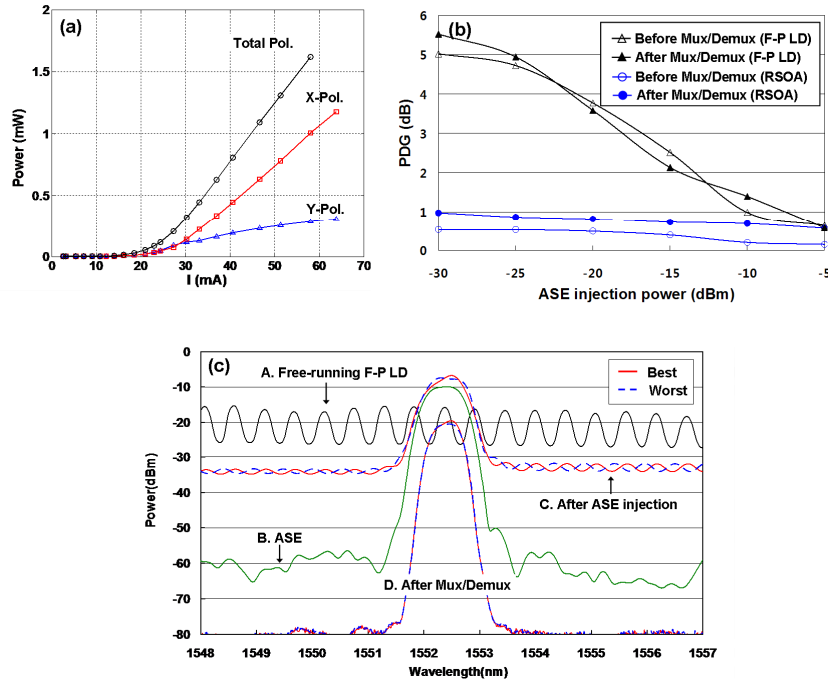


Fig. 3. Characteristics of PI F-P LD (a) L-I curve (b) PDG according to ASE injection power (c) measured spectra with ASE injection.

This feature is also clearly seen from the measured input and output spectrum of the PI F-P LD in Fig. 3(c). The free-running laser showed about 10 dB spectral ripple (spectrum A). However, it was reduced to less than 2 dB (spectrum C) both for the best case and the worst case at injection power of -4 dBm with the center wavelength of 1552.44 nm (spectrum B). At this injection power, the PDG was about 0.6 dB. Thus, we can consider the PI F-P LD as an RSOA with the PDG of 0.6 dB and spectral ripple of 2 dB [13]. To check the spectral characteristics of the F-P LD/RSOA, we measured the spectra according to the bias current and the temperature without the ASE injection as shown in Fig. 4. When we increased the bias current, the spectral ripple of the F-P LD was also increased (Fig. 4(a)). However, the ripple was less than 1 dB with increase of the bias current for the RSOA (Fig. 4(c)). This difference can be explained a very low anti-reflection coating of the RSOA. Both devices show similar temperature dependence as shown in Figs. 4(b) and 4(d). It may be noted again that the F-P LD is operating below the lasing threshold under the high ASE injection due to the deep depletion of the carrier density. It provides the reduction of the spectral ripple less than 2 dB as shown in Fig. 3(c) and Fig. 4(a).

We may recall the RIN as a function of the injection power in Fig. 2. When the injection power is low, the RIN of the RSOA is better than that of the F-P LDs. This is mainly due to high PDG of the F-P LDs. However, at high injection power, the PDG of the PI F-P LD decreases and the RIN becomes better than that of the RSOA, since there is resonant enhancement of the field for the PI F-P LD [14].

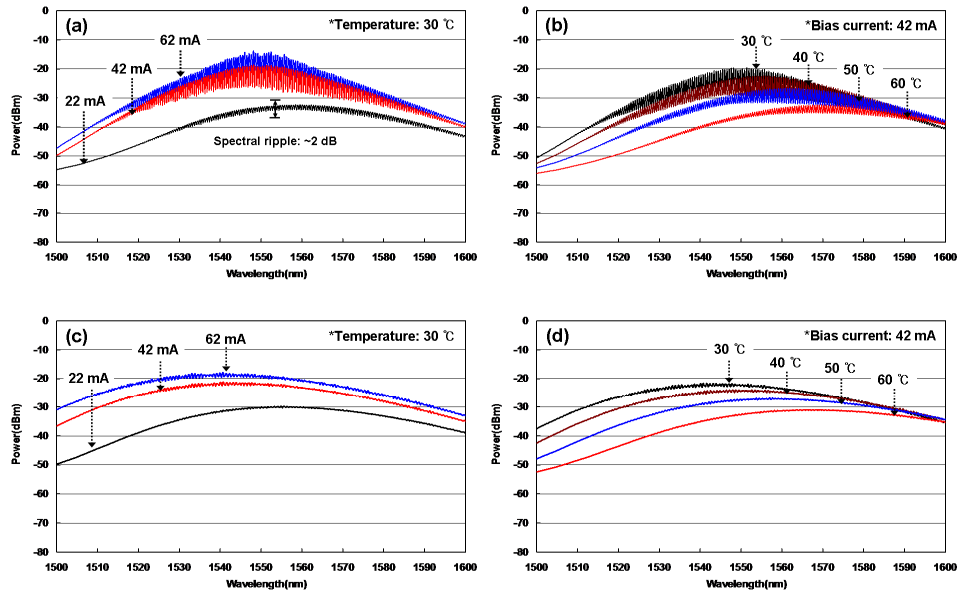


Fig. 4. Measured spectra according to (a) the bias current of the F-P LD (b) the ambient temperature of the F-P LD (c) the bias current of the RSOA (d) the ambient temperature of the RSOA.

3.3 Transmission of 2.5 Gb/s data

As seen in Fig. 2, we can use the PD F-P LD for 2.5 Gb/s transmission only for the best case. To confirm this, we measured bit error rate (BER) curves and RIN spectrum with an ASE injection power of -4 dBm at the back-to-back (B-t-B) configuration. The measured BER curves in Fig. 5(a) show an error-free transmission for the best case and an error-floor at the BER of 10^{-8} for the worst case as expected. For the best case, the measured RIN was -115 dB/Hz at low frequency. However, the RIN increases as increasing the frequency as shown in Fig. 5(b). This can be explained by a finite carrier lifetime of the F-P LD. For the worst case, the RIN was reduced only by 1.2 dB (-111.2 dB/Hz) compared with the spectrum-sliced ASE light (-110 dB/Hz). Thus, it is not sufficient to have BER less than 10^{-12} . These results imply that we need a forward error correction (FEC) or some signal processing to realize color-free operation with the PD F-P LD at 2.5 Gb/s per channel.

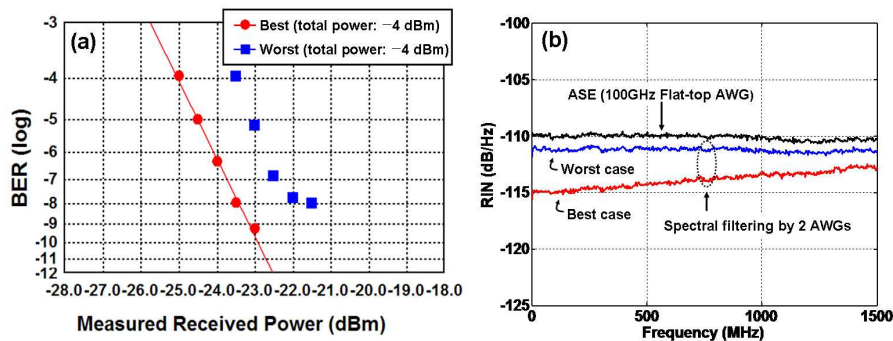


Fig. 5. Experimental results of PD F-P LD (a) measured BER curves (b) measured RIN.

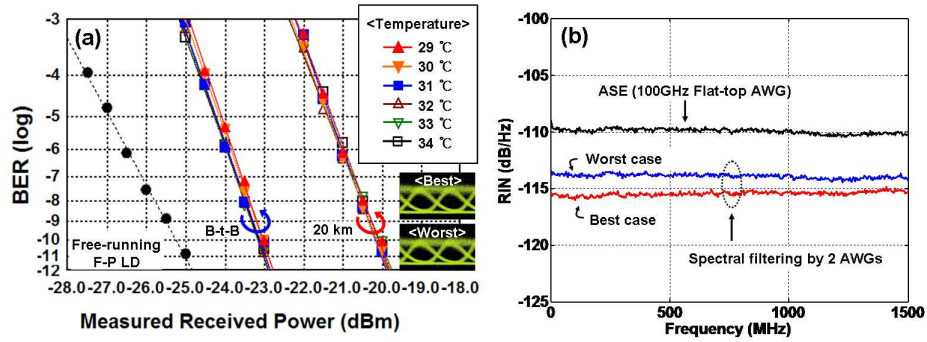


Fig. 6. Experimental results of PI F-P LD (a) measured BER curves (b) measured RIN.

Fortunately, the color-free operation can be achieved with the PI F-P LD, since we can reduce the RIN about 3 dB as shown in Fig. 2. This reduction of RIN directly comes from the use of both polarizations. To evaluate the system performance with the PI F-P LD, we measured the BER curves according to the detuning (or temperature) as shown in Fig. 6(a). Since the mode spacing of the F-P LD is 0.56 nm, the temperature change of 5 °C implies span of a mode spacing of the F-P LD. We achieved a color-free operation not only at the B-t-B condition, but also after 20 km transmission with the decision threshold control at the receiver. The inset shows the measured eye-diagrams of the best case and the worst case optical signal, respectively. As expected, the '1' level noise was broader than the '0' level noise because of the beat noise. The decision threshold level was set at the worst case of detuning (or RIN) to enhance the total system performance [9]. As a result, the similar BER performance was obtained regardless of the detuning. In Fig. 6(b), we also showed the measured RIN spectrum both for the best case and worst case of the wavelength-locked F-P LD after passing through the Mux/Demux. The RIN of the injected spectrum-sliced ASE was reduced about 16 dB (–126 dB/Hz) by the gain saturation effect of the PI F-P LD. However, the reduced RIN was increased to about 10.5 ~12 dB (–113.9 ~–115.5 dB/Hz) after passing through 2 AWGs. This is due to the optical filtering effects. The filtering of the wavelength-locked output brings about diminish of the noise suppression effects by reducing the correlation between the frequency components of the input light [12]. It should be noted that this filtering effect can be alleviated by placing an optical band-pass filter (pre-filter) having a narrow 3 dB bandwidth compared with that of AWG between a BLS and AWG [15].

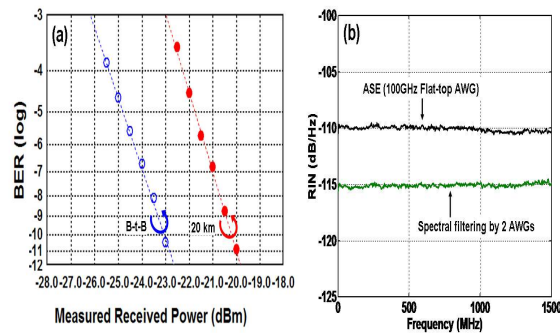


Fig. 7. Experimental results of PI RSOA (a) measured BER curves (b) measured RIN.

For comparison with the PI F-P LD, we also measured the BER curves and RIN with the PI RSOA. It was shown in Figs. 7(a) and 7(b), respectively. We achieved the similar experimental results compared with the PI F-P LD case as shown in Fig. 6. It shows an error-

free transmission with the reduced RIN of 5 dB. It may be noted again that the F-P LD suppressed the ASE beating noise more efficiently at the best case compared with the RSOA due to the cavity resonance characteristics at high injection power [14].

We have about 3 dB penalty after transmission of 20 km. To check the origin of this power penalty, we first measured BER curves as a function of the transmission length as shown in Fig. 8(a). We also calculated well-known dispersion penalty in Fig. 8(b). The 3-dB bandwidth of the wavelength-locked F-P LD output (for the widest case) was about 0.61 nm. The dispersion induced power penalty can be calculated by the below equation [16]

$$\Delta P_{\text{dispersion}} = -10 \log(1 - 5.1595 B^2 L^2 [0.18 \Delta \nu^2 D^2]) \quad (2)$$

where B is the data rate, L is the transmission length, $\Delta \nu$ is the equivalent source bandwidth and D is the chromatic dispersion. The term of $0.18 \nu^2 D^2$ in Eq. (2) represents the group delay variance. Based on the above equation, the calculated transmission length for 1-dB dispersion power penalty was about 20 km. However, the power penalty induced after 20 km transmission was much higher than the expected dispersion penalty and an error-floor was observed after 30 km transmission as shown in Fig. 8(a). This can be explained a de-correlation effect on the noise suppressed signal induced by the dispersion in transmission fiber [4,5]. It was confirmed by the measured RIN degradation of 0.8 dB and 1.7 dB after 20 km and 30 km transmission, respectively. It may be noted that for upstream transmission, we have additional penalty induced by optical back reflection. The estimated penalty with -32 dB back reflection was less than 0.6 dB due to broad bandwidth of signal [8].

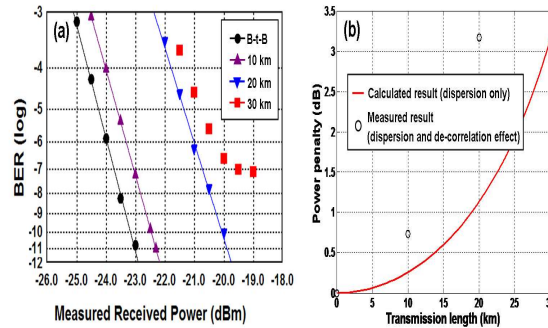


Fig. 8. Transmission results (a) measured BER curves and (b) calculated dispersion power penalty.

3.4 Demonstration of 80 Gb/s capacity WDM-PON

Based on the previous results, we demonstrated 32 channel WDM-PON with the PI F-P LD. Each channel conveys 2.5 Gb/s PRBS pattern length of 2^7-1 . The total ASE injection power into the F-P LD was varied from -4.3 dBm to -2.2 dBm channel by channel according to the different insertion loss of the AWG and the spectral profile of the BLS output. To confirm the color-free operation, we used a single transmitter for all 32 channels. The measured spectra of the free-running F-P LD and the wavelength-locked output of all 32 channels are shown in Figs. 9(a) and 9(b), respectively. The wavelength-locked spectra were measured at ONT after passing through 20 km fiber. The spectra show different shapes resulting from the different ASE injection power and the detuning. The inset of Fig. 9(b) shows the enlargement of locked spectra from channel 23 to channel 29. Then, we measured BER curves of all 32 channels as shown in Fig. 9(c). All BER curves show an error-free transmission which has the sensitivities ranged from -19.8 to -21.6 dBm at the BER of 10^{-12} . The maximum sensitivity difference between channels was about 1.5 dB. It implies the feasibility of color-free operation over

wavelength range of 1530-1560 nm. We also plotted the optical received power at the ONT in Fig. 9(d). The measured power was ranged from -15.7 dBm (minimum value at channel 1) to -13.5 dBm (maximum value at channel 31). If we consider the lowest receiver sensitivity of -19.8 dBm, the power margin of this WDM-PON system is more than 4 dB. It may be noted that the WDM-PON can be extended more than 32 channels because of the broad gain spectrum of F-P LD and the EDFA based BLS.

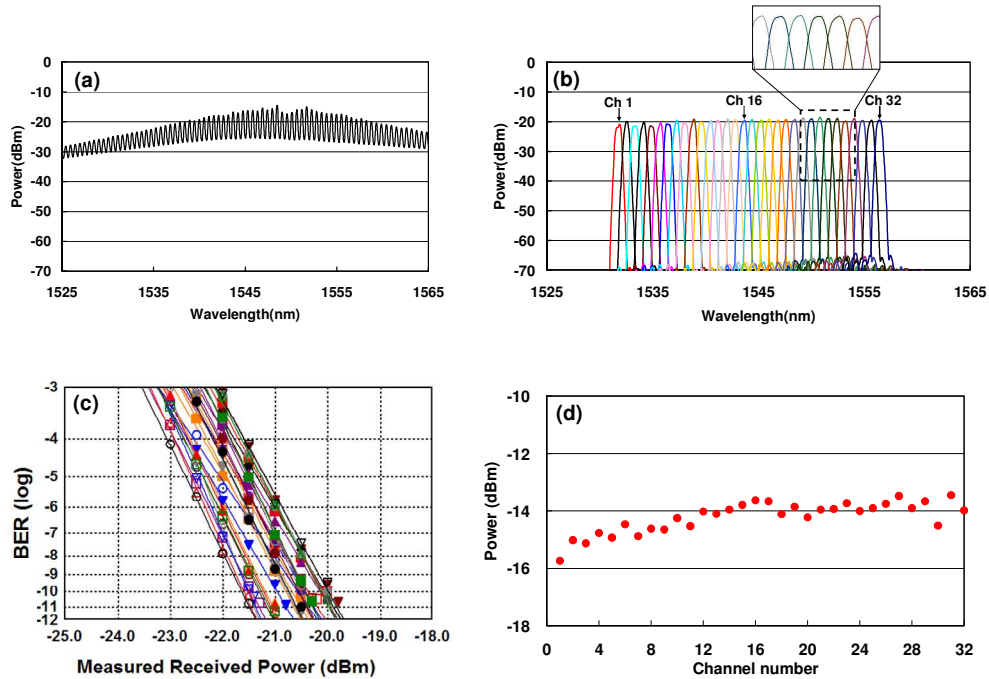


Fig. 9. (a) Spectrum of free-running PI F-P LD (b) Measured locked spectra (c) Measured BER curves after 20 km transmission of ch1~ch32 (d) Measured locked power of 32 channels at ONT.

4. Conclusion

We investigated 2.5 Gb/s per channel WDM-PON based on the wavelength-locked F-P LDs. The limitation resulting from the intensity noise was overcome by using the PI F-P LD. The PI F-P LD provides about 3 dB improved RIN compared with the PD F-P LD. Then, we demonstrated the color-free operation for an 80 Gb/s capacity WDM-PON with the transmission length of 20 km. In terms of transmission penalty, the phase de-correlation of the noise suppressed signal was a dominant source. In addition, we also compared the characteristic of the PI F-P LD with that of the RSOA. The performance of the F-P LD was similar to that of the ROSA. However, a simple device structure of the F-P LD can provide a high packaging yield compared with the RSOA.